AAPS PharmSciTech

Near-Infrared Spectral Imaging for Quality Assurance of Pharmaceutical Products: Analysis of Tablets to Assess Powder Blend Homogeneity

Submitted: April 19, 2002; Accepted: July 1, 2002

Robbe C. Lyon[1], David S. Lester[2], E. Neil Lewis[3], Eunah Lee[3], Lawrence X. Yu[1], Everett H. Jefferson[1] and Ajaz S. Hussain[4]

[1]Division of Product Quality Research, Food and Drug Administration, Kensington, MD 20895
[2]Pharmacia Corporation, 100 Rt 206 North, Peapack, NJ 07977
[3]Spectral Dimensions, Inc, 3416 Olandwood Court, Suite 210, Olney, MD 20832
[4]Office of Pharmaceutical Sciences, Food and Drug Administration, Rockville, MD 20857

ABSTRACT The objective of this study was to evaluate near-infrared (NIR) spectroscopic imaging as a tool to assess a pharmaceutical quality assurance problem - blend uniformity in the final dosage product. A system based on array detector technology was used to rapidly collect high-contrast NIR images of furosemide tablets. By varying the mixing, 5 grades of experimental tablets containing the same amount of furosemide and microcrystalline cellulose were produced, ranging from well blended to unblended. For comparison, these tablets were also analyzed by traditional NIR spectroscopy, and both approaches were used to evaluate drug product homogeneity. NIR spectral imaging was capable of clearly differentiating between each grade of blending, both qualitatively and quantitatively. The spatial distribution of the components was based on the variation or contrast in pixel intensity, which is due to the NIR spectral contribution to each pixel. The chemical nature of each pixel could be identified by the localized spectrum associated with each pixel. Both univariate and partial least squares (PLS) images were evaluated. In the suboptimal blends, the regions of heterogeneity were obvious by visual inspection of the images. A quantitative measure of blending was determined by calculating the standard deviation of the distribution of pixel intensities in the PLS score images. The percent standard deviation increased progressively from 11% to 240% from well blended to unblended tablets. The NIR spectral imaging system provides a rapid approach for acquiring spatial and spectral information on pharmaceuticals. The technique has potential for a variety of applications in product quality assurance and could affect the control of manufacturing processes.

Key Words: NIR imaging, chemical imaging, NIR spectroscopy, blend uniformity, quality assurance

***Corresponding Author:** Robbe C. Lyon, FDA, CDER, DPQR, HFD-941, Nicholson Research Center, 5600 Fishers Lane, Rockville, MD 20857. Telephone: 301-827-5246; Facsimile: 301-594-6289; E-mail: lyonr@cder.fda.gov

INTRODUCTION

Pharmaceutical quality control and quality assurance depend on monitoring the composition and uniformity of the drug substance during processing and in the final product. Compendial tests have traditionally been used to determine identity, strength, quality, and purity. Vibrational spectroscopic techniques, including mid-infrared, near-infrared (NIR), and Raman, have been proposed as alternative approaches [1,2]. Implementation of these approaches can reduce the time and resources required for manufacturing, while improving quality control. These spectroscopic methods provide physical as well as chemical characterization of the active and inactive components in composite mixtures. NIR spectroscopy has been utilized to determine the homogeneity of pharmaceutical powder blends [3] and to monitor powder blending processes online [4-6].

However, traditional spectroscopy (single-point, bulk spectroscopy) cannot directly determine the spatial distribution of the components in the final product. To accomplish this, an imaging technique is necessary to map the location of each spatially resolved component.

The combination of digital imaging and molecular spectroscopy for the molecular analysis of compounds is referred to as chemical imaging. Initially, Raman imaging [7,8] and infrared imaging [8-10] were achieved by scanning techniques. Various mapping techniques were coupled with traditional single-point vibrational spectroscopy to produce sample visualization. This approach is time consuming and requires mechanical movement of the sample. Recently, high-resolution multispectral imaging has been achieved by passing the image light through a tunable filter [11]. This approach bypasses the problems associated with single-point mapping and simultaneously reveals the type, distribution, and relative abundance of chemical components within a particular system. The image array is then captured for Raman imaging [12,13] by a silicon charged-coupled device detector or for infrared imaging [14-15] by a focal plane array (FPA) detector. Additionally, for infrared chemical imaging, light may be modulated by an interferometer instead of a tunable filter [16-17]. The visualization of the internal structure of pharmaceutical tablets has recently been demonstrated by NIR imaging [18] and Raman imaging [19,20]. NIR imaging has also been used to monitor powder blend homogeneity online [6].

The objective of this study was to evaluate NIR spectroscopic imaging as a tool to assess a pharmaceutical quality assurance problem - blend uniformity in the final dosage product. In this study, the blend uniformity of furosemide and microcrystalline cellulose was determined by evaluating the finished tablets by NIR imaging and by traditional NIR reflectance spectroscopy. Intact tablets requiring no sample preparation were rapidly and noninvasively analyzed by both approaches. Experimental tablets were designed to deliberately vary the homogeneity of the components. The grades of tablets were differentiated quantitatively by NIR spectral imaging and by traditional NIR spectroscopy. In addition , NIR spectral imaging provided a visual distribution of components within each tablet. Each grade of tablet was clearly differentiated. This study demonstrates the power of this new imaging tool for assessing pharmaceutical quality assurance.

METHODS

NIR Spectral Imaging

The image data sets of intact pharmaceutical tablets were collected by the MatrixNIR^{TM} NIR Spectral Imaging System (Spectral Dimensions, Inc, Olney, MD) shown as a block diagram in Figure 1. The imaging system consists of a liquid crystal tunable filter (LCTF) coupled with an NIR sensitive FPA detector. The diffuse reflectance image of the sample is passed through the LCTF. For this particular study, the tunable filter element rapidly selects wavelengths at selected nm intervals over a spectral range of 1000-1700 nm. A series of images are then captured by the indium-gallium-arsenide near-infrared FPA detector with a total acquisition time of approximately 2 minutes. Each pixel in the detector array corresponds to an approximately 1600 μm^2 (40 μm x 40 μm) area of the sample surface, and the resulting data set contains 71 wavelength increment scans per spectrum. The array contains 320 x 240 pixels or 76,800 equivalent spectra. The data sets are generally referred to as image cubes or hyperspectral image cubes. Detecting data in this manner, the spectroscopic imaging technique bypasses the problems associated with single-point mapping and simultaneously reveals the type, distribution, and relative abundance of chemical components within a particular system. This is achieved with a system that contains no moving parts.

The vibrational spectra collected for each pixel on the array detector create a third dimension. The 3-dimensional cube (shown in Figure 2) consists of both spatially resolved spectra and wavelength-dependent images. The X and Y axes represent spatial information, and the Z axis represents reflectance at the selected NIR wavelengths. The image

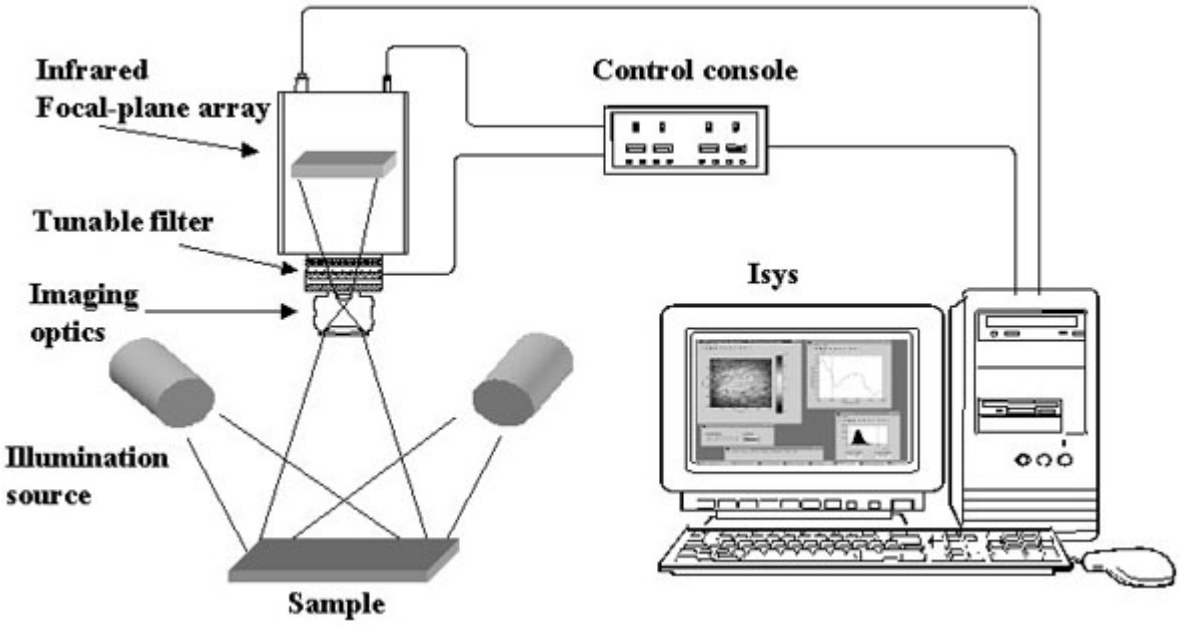

Figure 1. Simplified block diagram of the MatrixNIR™ NIR spectral imaging system.

cube can be seen as a series of wavelength-resolved images or, alternatively, as a series of spatially resolved spectra, one for each point on the image. The complete integration of spatial and spectral information adds a new dimension to data analysis. The ability to explore the interdependency of spectral and spatial information is the basis for its unique capabilities that differ qualitatively from simple point-by-point spectroscopy. Effectively mining the immense volume of chemical and spatial information contained within the data of spectroscopic images requires multivariate analysis methodologies.

Data were analyzed using ISys™ (Spectral Dimensions, Inc), a graphical user interface, and an integrated software package designed specifically for the acquisition, visualization, and analysis of hyperspectral image cubes and maps. Localized NIR spectra associated with each pixel and images associated with each NIR wavelength are readily displayed. The software package contains standard spectral analysis and image analysis tools as well as advanced chemometric qualitative and quantitative analysis capabilities.

Based on processing, 2 types of images are shown in this study: univariate images and partial least squares (PLS) score images. For all images, a Spectralon (Labshere, Inc, North Sutton, NH) background image cube was used to correct both the spatial and spectral response of the system; all images were preprocessed by taking the inverse common logarithm to convert to log (1/R). The univariate images were generated by additional preprocessing using normalization (division of the image cube by a selected image plane) to enhance the contrast. To observe a spatial image plane from the image cube, a wavelength is selected. The intensity of each pixel in that spatial image plane is the intensity of the NIR spectrum at that wavelength. The complete, localized NIR spectrum can be observed by selecting any pixel in the spatial plane. PLS score images were generated using PLS analysis type 2. The initial preprocessing also included a linear baseline correction. A library was built from the pure component spectra representing this binary system (furosemide and Avicel). The spectral absorbance for each pixel was decomposed into score values associated with each component. The intensity values for the PLS score images shown represent the score values for class 1, furosemide.

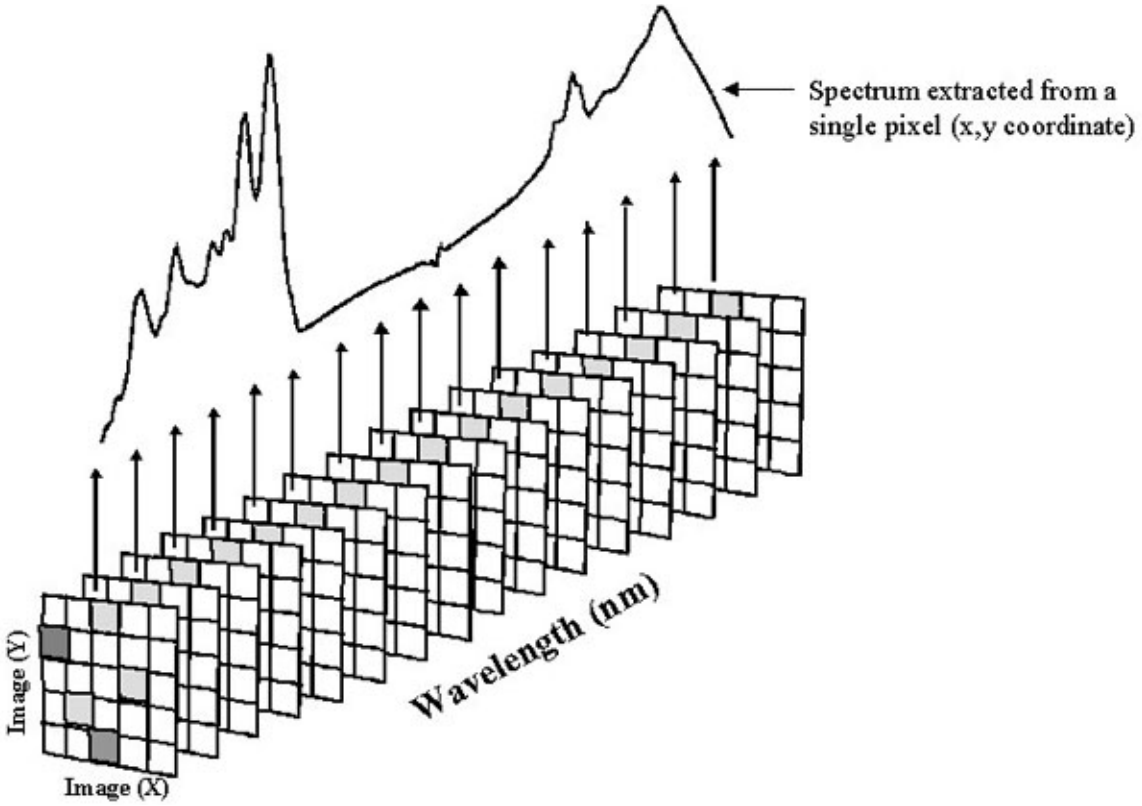

Figure 2. A schematic of the spectral hypercube. Each pixel is spatially located in the X-Y image plane. A representative NIR spectra associated with one pixel is shown in the third dimension.

Traditional NIR Spectroscopy

In addition to NIR spectral imaging, intact pharmaceutical tablets were scanned by NIR spectroscopy. Reflectance spectra were collected using a Foss NIRSystems Model 6500 spectrometer (Foss NIRSystems, Inc, Silver Spring, MD) equipped with a NIRSystems rapid content analyzer containing a tablet holder. The top and bottom surfaces of each tablet were scanned over the range of 1100-2500 nm to generate a bulk average NIR spectrum for each tablet surface. Each spectrum was time averaged from 32 scans generated at 0.6 scans/sec. The background reference was a 1" diameter Spectralon 99% reference reflectance plate (Labsphere, Inc, North Sutton, NH).

Statistical Analysis of Tablet Variability

The blend uniformity in the tablets could be determined qualitatively from the NIR images by visual inspection. A quantitative measure was established by calculating the % standard deviation of the distribution of pixel intensities as represented by the histograms of the PLS score images. The blend uniformity in the tablets was also estimated from traditional NIR spectroscopy by evaluating the consistency of the reflectance NIR spectra. The measures of the intra-tablet variability and the inter-tablet variability were determined from the average % standard deviations in the NIR spectra. An average % standard deviation was calculated by averaging the % standard deviations (relative to the mean intensity value) of 20 spectral peaks in a set of second-derivative NIR spectra. These 20 spectral peaks represented the major contributions from furosemide and Avicel. For the intra-tablet variability, the set consisted of 2 second-derivative spectra for each tablet (one from side 1 and one from side 2).

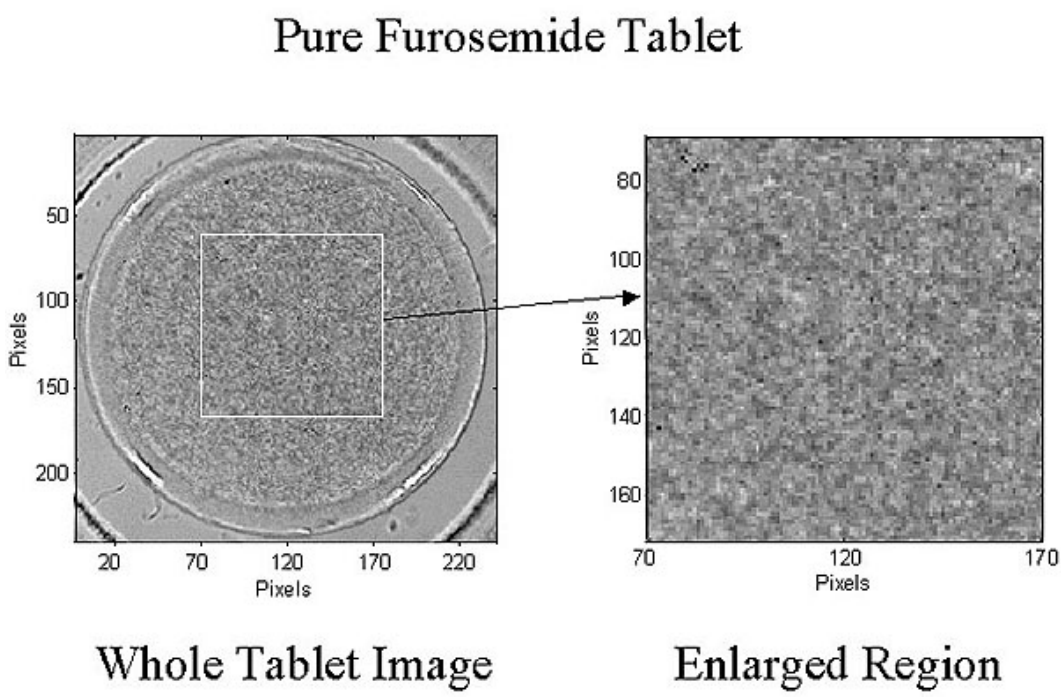

Figure 3. NIR chemical image of whole tablet of pure furosemide and enlargement of the 100 × 100 pixel region analyzed.

The average % standard deviation was calculated for each tablet. This value was averaged for each group (n = 3). For the inter-tablet variability, the set consisted of 3 second-derivative spectra from one side of each tablet in a blend group. An average % standard deviation was calculated for side 1, and this was averaged with an average % standard deviation calculated for side 2.

Pharmaceutical Samples

Both experimental and commercial-grade furosemide tablets containing 80 mg furosemide and 240 mg excipient mix (99.67% Avicel PH 102 and 0.33% magnesium stearate) were evaluated. The experimental tablets differed in the degree of blending. The homogeneity was controlled by varying the mixing time. The content uniformity for the experimental tablets was controlled by individually weighing the raw materials for each tablet. Experimental tablets were individually prepared by adding 80.0 mg furosemide to 240.0 mg excipient mix, hand blending, and direct compression using a Carver Press. Five groups of experimental tablets (Blends A, B, C, D, and E) were prepared, ranging from well blended to unblended. In addition, reference tablets containing pure furosemide and reference tablets containing only excipient mix were individually prepared. The commercial-grade furosemide tablets were manufactured at the University of Iowa. These were prepared in bulk by machine blending and direct compression using an automated tablet press. The content uniformity for the commercial-grade tablets was determined using USP assay procedures.

RESULTS

The NIR spectral image of a whole tablet (pure furosemide) is shown in Figure 3. The enlarged region represents the area (100 x 100 pixels) shown in subsequent tablet images. The reference tablets con

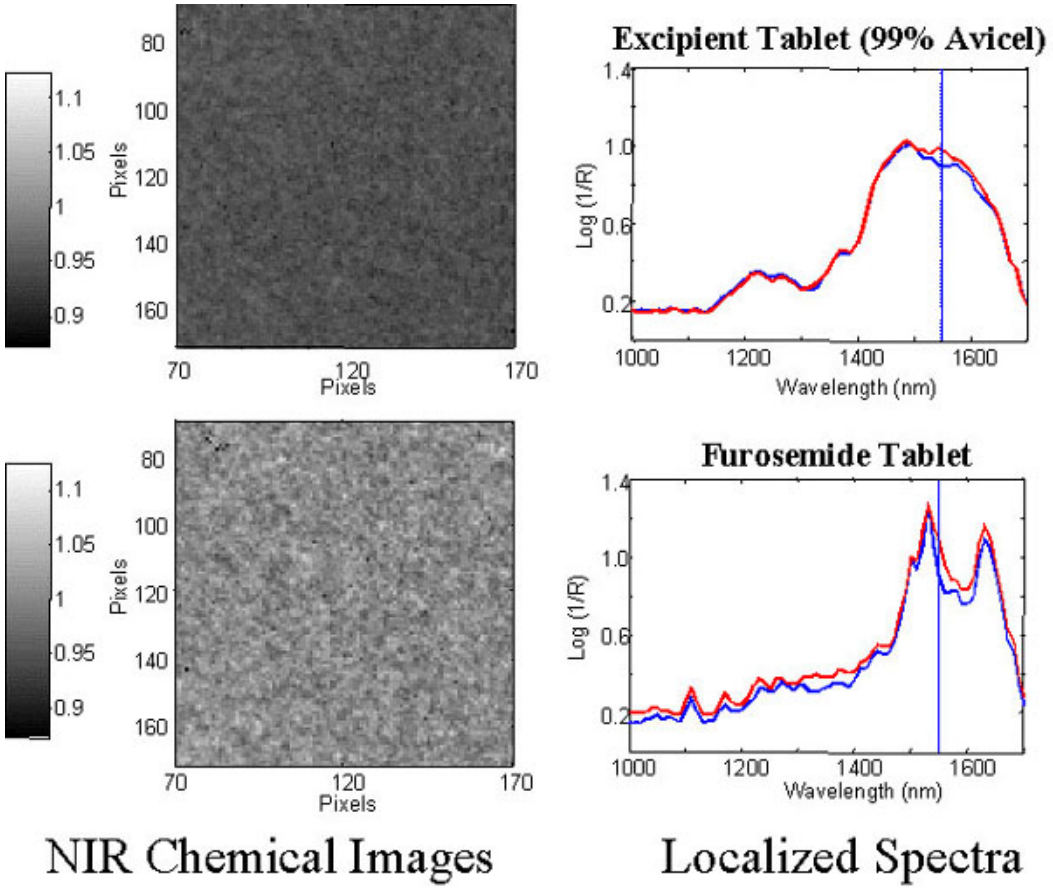

Figure 4. NIR univariate images (at 1540 nm image plane) and localized spectra of tablet containing only excipient mix and tablet of pure furosemide. The red spectrum is generated from the highest intensity pixel, and the blue spectrum is generated from the lowest intensity pixel in each image field.

taining pure furosemide and reference tablets containing only excipient mix were imaged to generate spectral characteristics of each component.

Representative univariate images and associated localized spectra are shown in Figure 4. Each NIR spectrum displayed excellent signal-to-noise characteristics. A slightly different localized NIR spectrum is associated with each pixel. Two spectra are shown for each image. One is generated from the lightest pixel in the field and the other from the darkest pixel in the field. For these reference tablets, each pixel in the image field contained the same spectral character. The image contrast is due primarily to slight differences in overall intensity, rather than variations in the character of the spectra.

NIR univariate images and representative spectra of the commercial-grade tablets and the 5 experimental tablets are shown in Figures 5-7. The image contrast is a function of the intensity of the NIR spectrum associated with each pixel at a specified wavelength. The image planes at a wavelength of 1626 nm were selected to maximize the image contrast. The 6 univariate images in Figures 5-7 were processed together and were normalized to the same contrast scale. Each pixel contains spectral contributions from furosemide and excipients as indicated by the color scale. The dark red represents pure furosemide and the dark blue represents pure excipient. As a result, the spatial distribution of the furosemide and excipients are visualized. This is an excellent way to "mine" both spatial and chemical variance within the sample.

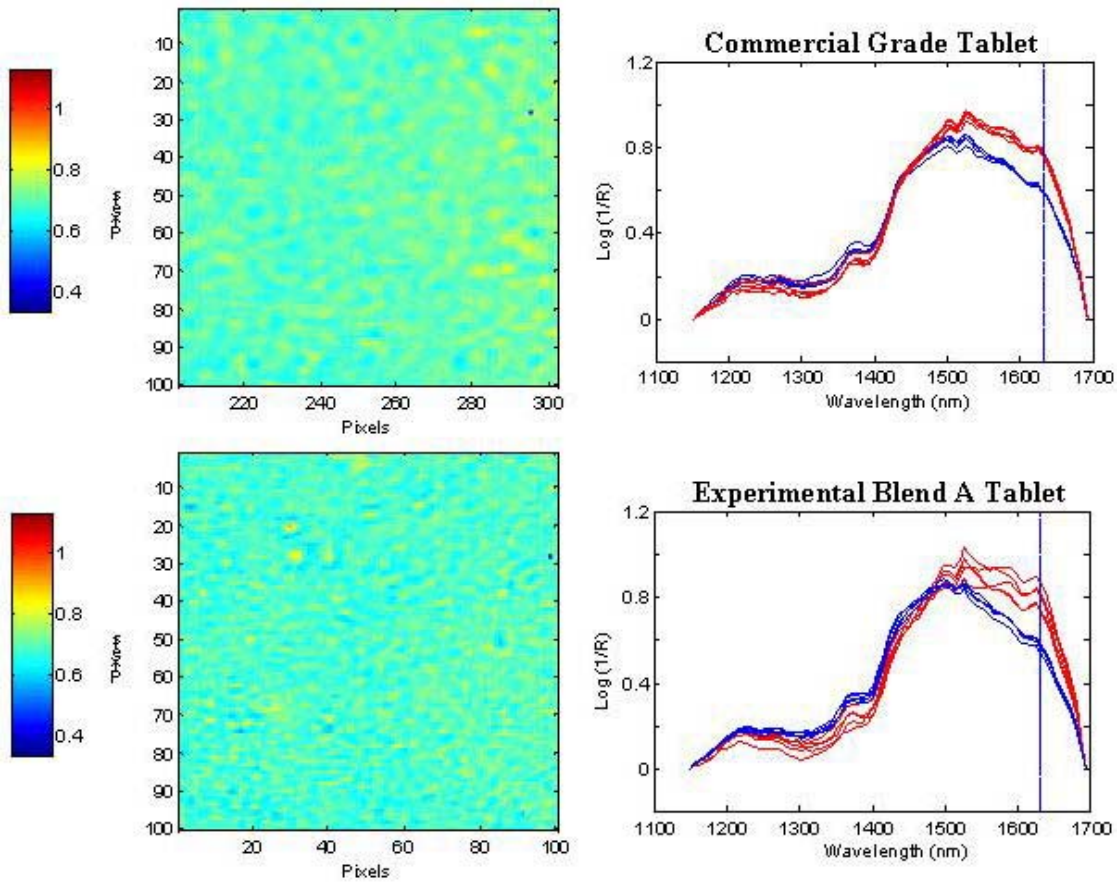

Figure 5. NIR univariate images (at 1626 nm image plane) and localized spectra of the well-blended tablets: commercial-grade tablets and Blend A tablets. The red spectra are generated from the 5 highest intensity pixels and blue spectra from the 5 lowest intensity pixels in each image field. The same intensity scale is used for Figures 5-7 with the highest intensity representing furosemide and the lowest intensity representing excipients.

The well-blended tablets (commercial-grade and Blend A) are shown in Figure 5. The images show a uniform distribution of components and a minimum of contrast. Consequently there was little difference between representative spectra collected from the low-intensity and high-intensity pixels. The enriched spectral character of furosemide in the high-intensity pixels in Blend A tablets indicates that this blend is slightly less homogeneous than the commercial-grade tablets.

The images of the tablets prepared from Blends B, C, D, and E show a progressive increase in heterogeneity. The results from the moderately blended tablets are shown in Figure 6. Small clusters of high-intensity pixels are evident in the images of Blend B tablets. The corresponding spectra indicate that these pixels are enriched with furosemide. Small clusters of higher intensity pixels are evident in the images of Blend C tablets. The corresponding spectra indicate that these pixels are nearly pure furosemide. The results from the poorly blended tablets are shown in Figure 7. Large domains of pure furosemide and excipient characterize the images of Blend D tablets. As expected, the components are completely separated in the images of Blend E tablets. The images clearly distinguish the degree of blend uniformity in accordance with the degree of

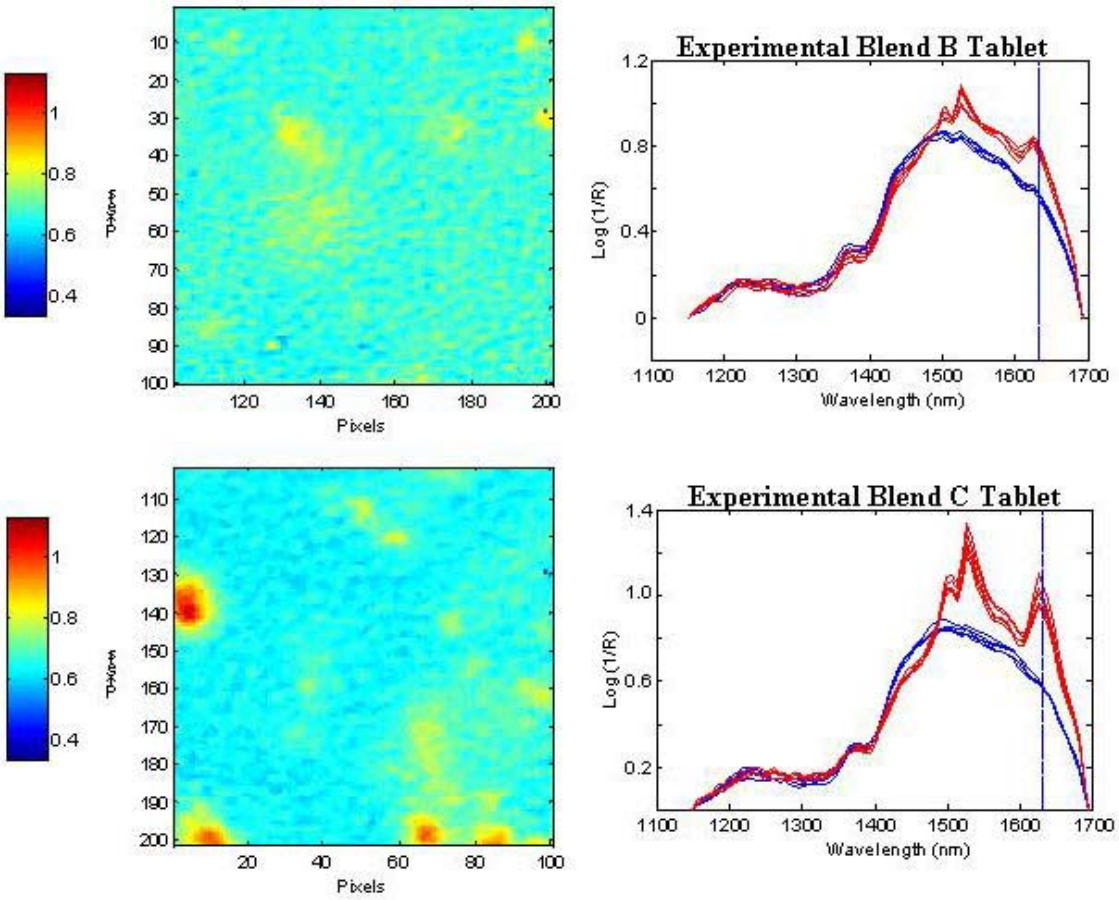

Figure 6. NIR univariate images (at 1626 nm image plane) and localized spectra of the moderately blended tablets: Blend B tablets and Blend C tablets. The red spectra are generated from the 5 highest intensity pixels and blue spectra from the 5 lowest intensity pixels in each image field.

blending. The spectra identify the relative chemical composition of each pixel.

PLS score images of the commercial-grade tablets and the 5 experimental tablets are shown in Figures 8 to 10. The corresponding histograms represent distribution of pixel values about a mean value based on class 1 (furosemide). Greater contrast is observed in these images compared to the NIR univariate images. The well-blended tablets (commercial-grade and Blend A) are shown in Figure 8. Like the univariate images, these images show a uniform distribution of components and a minimum of contrast. A slight heterogeneity is observed in the image of the Blend A tablet (2 small clusters of high-intensity pixels) that was not obvious in the univariate image. Both histograms exhibit a symmetric distribution. The high-intensity and low-intensity pixels contribute to the slight extension in tailing of the histogram distribution for Blend A tablets that was not observed in the histogram of the commercial-grade tablet.

The results from the moderately blended tablets are shown in Figure 9. A slight asymmetry of the histogram distribution for Blend B tablets is perceptible because of the clusters of high-intensity pixels representing enriched furosemide. The histogram

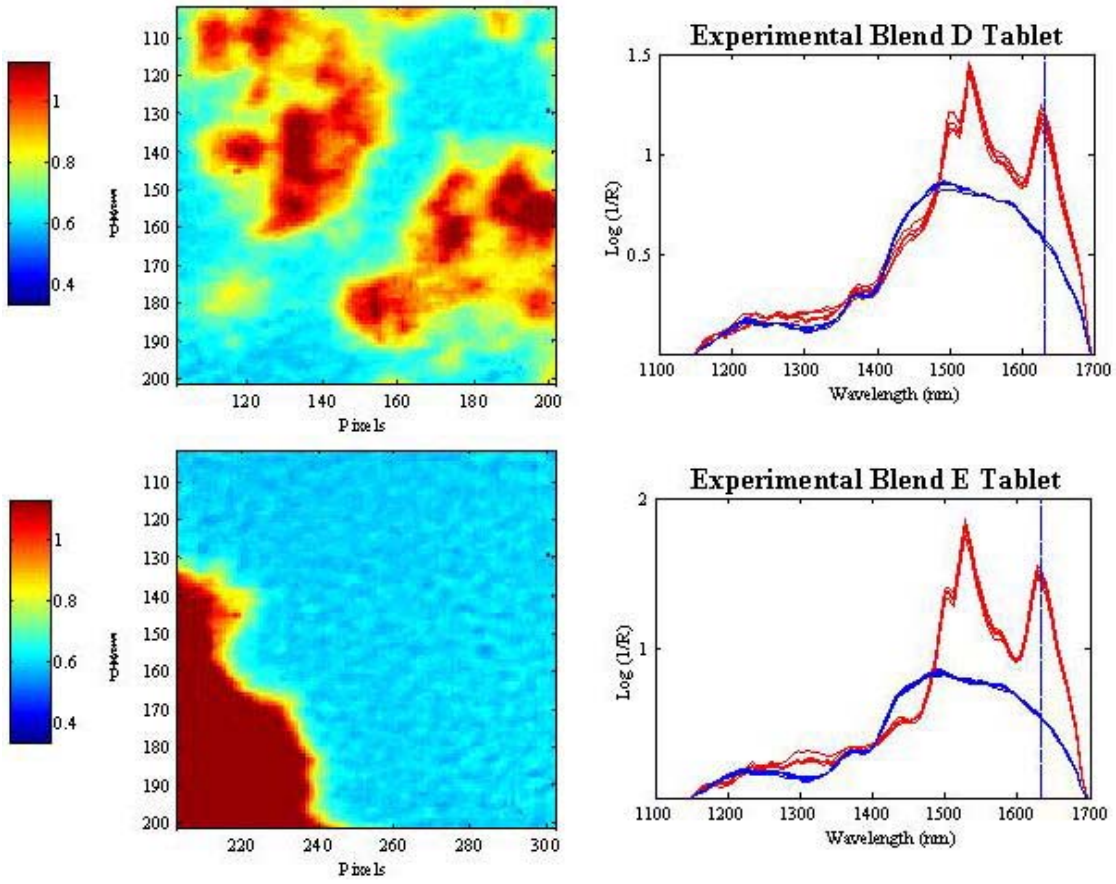

Figure 7. NIR univariate images (at 1626 nm image plane) and localized spectra of the poorly blended tablets: Blend D tablets and Blend E tablets. The red spectra are generated from the 5 highest intensity pixels and blue spectra from the 5 lowest intensity pixels in each image field.

distribution for Blend C tablets is more asymmetric. The mode of the distribution has clearly shifted to a lower value, indicating a diminished furosemide concentration in the majority of the pixels. The population of high scores corresponds with clusters of pixels representing nearly pure furosemide.

The results from the poorly blended tablets are shown in Figure 10. The histogram for Blend D tablets is nearly a bimodal distribution. Although the 2 populations are poorly resolved, there is a population low in furosemide and a population high in furosemide. The histogram for Blend E tablets is clearly a bimodal distribution. The mode of the larger population occurs at zero, indicating that these pixels are devoid of furosemide contributions. The furosemide-enriched population is broadly distributed because of the diffuse interface between active and excipient.

The width of the distribution shown in each histogram is an indicator of the heterogeneity of furosemide in that tablet. The standard deviation of the population was used as a quantitative measure of the tablet uniformity. A statistical evaluation of the % standard deviations (relative to the mean) of the histograms generated by the PLS score images is shown in Table 1. The % standard deviation of

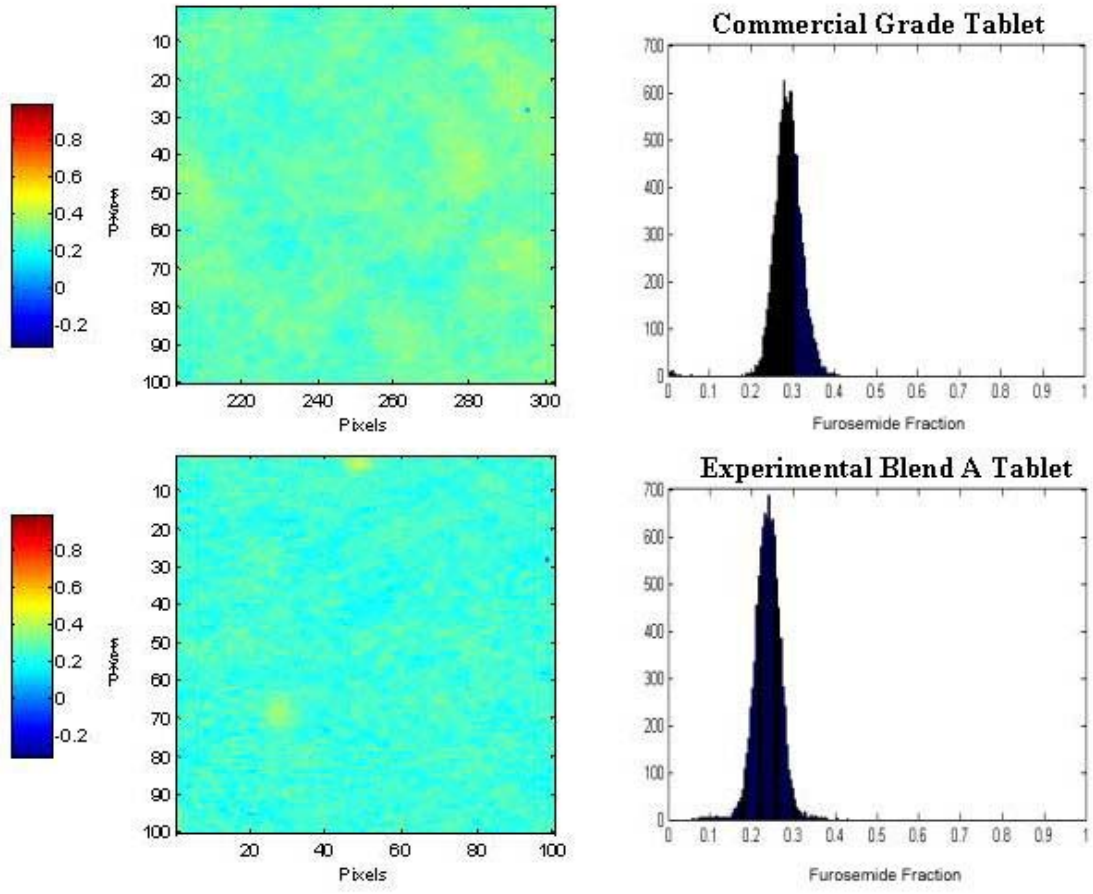

Figure 8. NIR PLS score images and associated histograms of the well-blended tablets: commercial-grade tablets and Blend A tablets. The same intensity scale is used for Figures 8-10, with the highest intensity representing furosemide and the lowest intensity representing excipients.

the histogram distribution for each tablet and the average % standard deviation for the 3 tablets in each group are presented. There was no statistical difference between the average % standard deviation for the commercial tablets (11.0 ± 1.9) and the Blend A tablets (11.7 ± 1.6). A progressive increase in the average % standard deviation was observed as the degree of blending declined.

For comparison with NIR spectral imaging, the commercial-grade tablets and the 5 experimental tablets were also evaluated by traditional NIR spectroscopy. The top and bottom surfaces of each tablet were scanned to generate a bulk average NIR reflectance spectrum for each tablet surface. For illustration, the NIR spectra (second derivative) of well-blended tablets (3 Blend A) and the worst-blended tablets (3 Blend E,) are shown in Figure 11.

The degree of heterogeneity associated with each grade was assessed by evaluating intra-tablet and inter-tablet variability. The methods for calculating each are described in detail in the methods. In general, the variability was determined by comparing second derivative spectra and calculating % standard deviations (relative to the mean). The measure of intra-tablet variability was the % standard deviation of the second-derivative spectrum between side

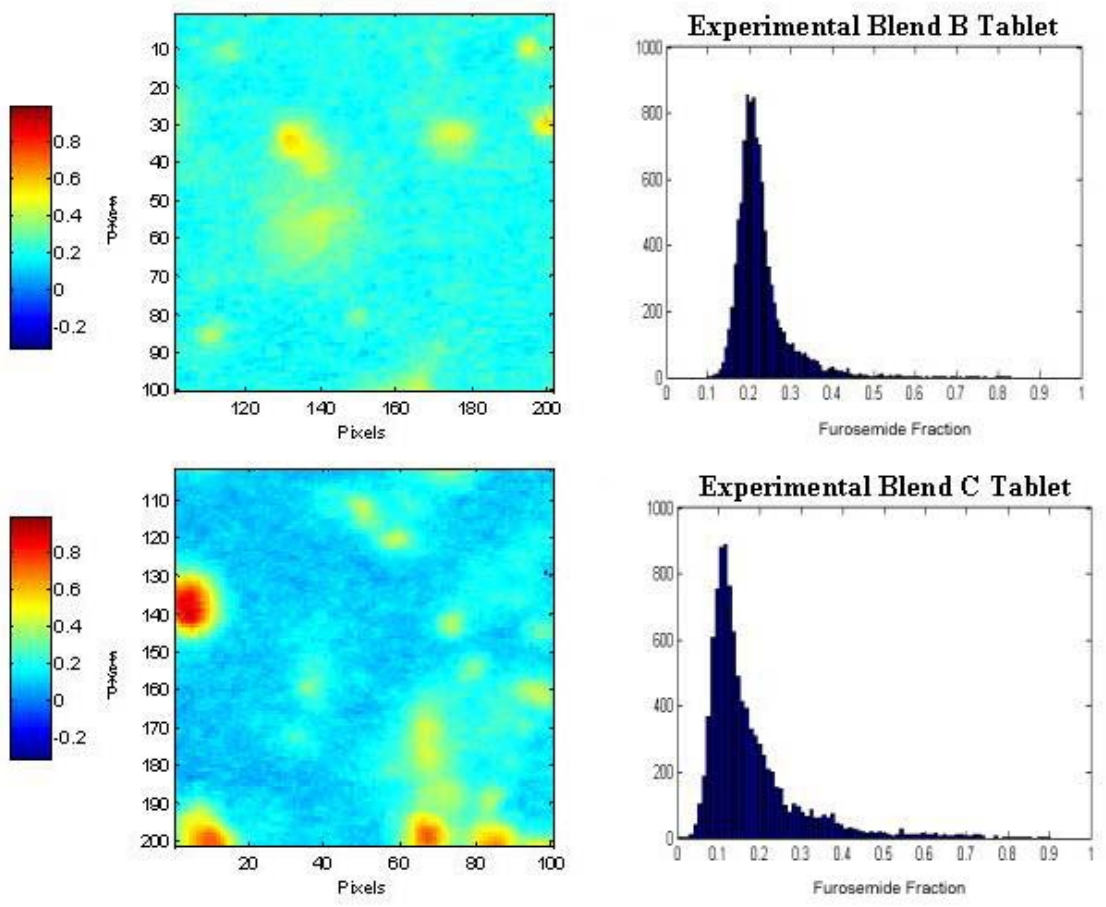

Figure 9. NIR PLS score images and associated histograms of the moderately blended tablets: Blend B tablets and Blend C tablets.

1 and side 2 of each tablet. The average % standard deviation was calculated for each group. The results are summarized in Table 2.

The intra-tablet variability progressively increased as the degree of blending declined (with exception of Blend E tablets). The measure of inter-tablet variability was the average of the % standard deviation of side 1 and the % standard deviation of side 2 of the 3 tablets in each group. The results are summarized in Table 3. The inter-tablet variability progressively increased as the degree of blending declined.

DISCUSSION

In this study, NIR spectral imaging and traditional NIR spectroscopy have been utilized as end-product tests. Homogeneity testing of the drug product complements blend analysis. Blend uniformity testing provides feedback to assist in the process development, while the end-product test provides assurance that the blend remained uniform during processing. This is consistent with the Product Quality Research Institute Blend Uniformity Working Group document proposed to demonstrate adequacy of mix by stratified sampling of blend and dosage units [21].

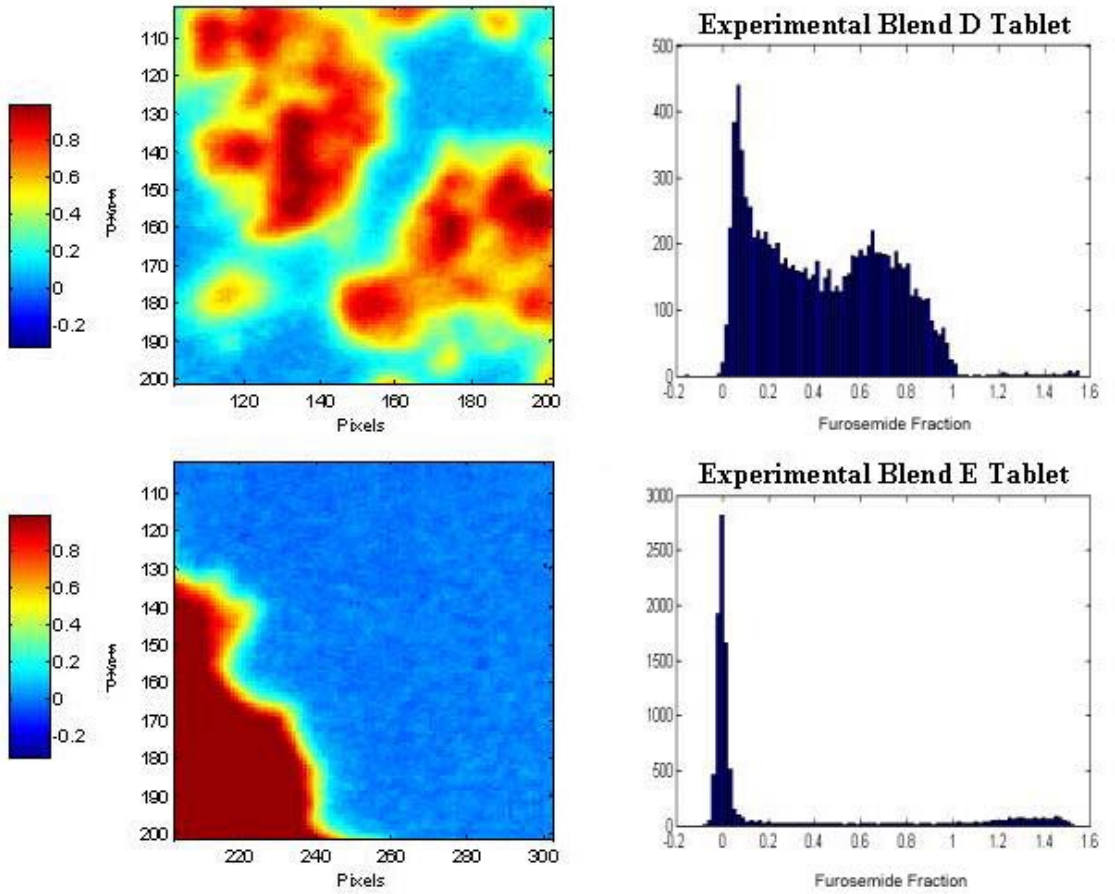

Figure 10. NIR PLS score images and associated histograms of the poorly blended tablets: Blend D tablets and Blend E tablets.

Table 1. Variability of Histogram Distributions from PLS Score Images. % Standard Deviations (%SD) of Histogram Distributions from PLS Score Images

Blend	Tablet 1	Tablet 2	Tablet 3	Average %SD
Commercial	11	13	9	11
A	12	10	13	12
B	25	18	33	25
C	67	64	80	71
D	121	119	93	111
E	203	251	268	240

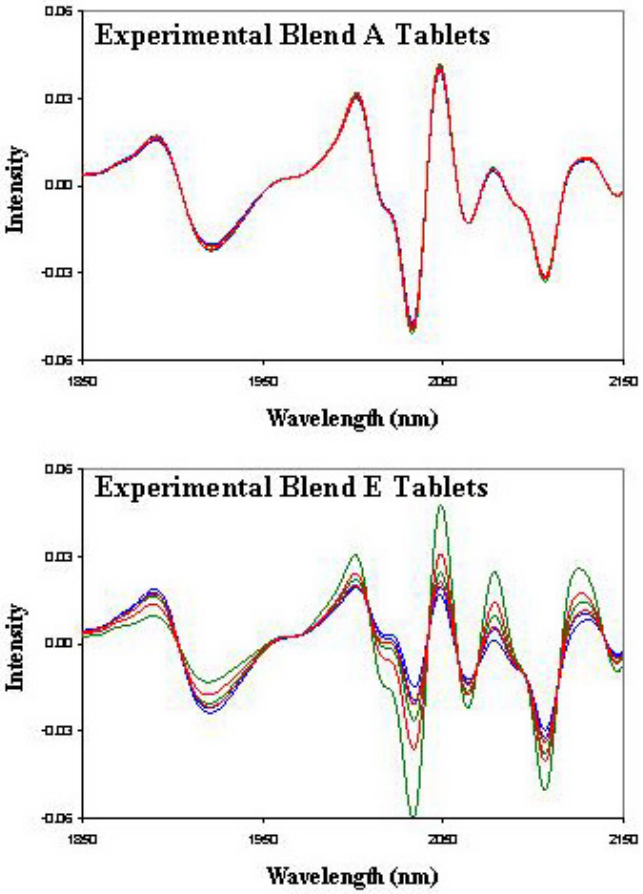

Figure 11. Traditional NIR spectra of each side of 3 Blend A tablets and 3 Blend E tablets. For clarity, only a selected wavelength region (1850-2150 nm) of the second derivative spectra is shown. For each group, tablet 1 is represented by green, tablet 2 is represented by red, and tablet 3 is represented by blue.

Table 2. Intra-tablet Variability of Second Derivative Spectra from NIR Spectroscopy. % Standard Deviation (%SD) between Side 1 and Side 2 for Each Tablet

Blend	Tablet 1	Tablet 2	Tablet 3	Average %SD
Commercial	0.3	0.4	0.4	0.4
A	2.8	1.9	2.5	2.4
B	7.1	4.2	4.9	5.4
C	24	14	6.9	15
D	52	12	12	25
E	25	5.5	12	14

NIR spectral imaging was capable of assessing the quality of tablet blend uniformity both qualitatively and quantitatively. The spatial uniformity of the components could be ascertained qualitatively by visual inspection of the images. In the suboptimal blends, the regions of heterogeneity were obvious. The degree of blending was quantitated by statistical analysis of the pixel compositions. In the well-blended tablets, all pixels had nearly the same composition, as represented by a narrow distribution of pixel values. As the tablets became less uniform, the distribution of pixel values broadened until the distribution separated into 2 distinct classes. The subtle differences between the well-blended tablets, the commercial-grade tablets, and the Blend A tablets could be distinguished only by visual observation (clustering of components) and not by statistical analyses.

Table 3. Inter-tablet Variability of Second Derivative Spectra from NIR Spectroscopy. % Standard Deviation (%SD) of Side 1 and Side 2

Blend	Side 1	Side 2	Average %SD
Commercial	2.1	2.3	2.2
A	3.1	2.1	2.5
B	3.8	3.0	3.4
C	8.1	15	12
D	6.8	27	17
E	29	16	23

Traditional NIR spectroscopy was limited in its ability to evaluate drug product homogeneity. The qualitative aspect associated with mapping the spatial distribution is lacking with this approach. The assessment of tablet uniformity was dependent on the statistical comparisons of NIR spectra from the same tablet and tablets in the same group. The assumption is made that the combination of intra-tablet variability and inter-tablet variability translates into a measure of blend uniformity. The intra-tablet variability and inter-tablet variability increased with tablet heterogeneity. The intra-tablet variability was capable of distinguishing each tablet grade except the Blend E tablets. The average % standard deviation associated with intra-tablet variability was lower than expected for the Blend E tablets. These unblended tablets were prepared by placing the components side by side. The similarity between side 1 and side 2 may be due to this plane of symmetry. The inter-tablet variability increased progressively with tablet heterogeneity.

Compared to traditional NIR spectroscopy, NIR spectral imaging provides the opportunity to investigate localized microdomains within a drug product. A physical or chemical abnormality that makes a minimal contribution to the bulk tablet may go undetected by traditional NIR spectroscopy. The same abnormality could dominate a microdomain and be detected in the NIR image.

The NIR spectral imaging system provides a rapid approach for acquiring high-resolution spatial and spectral information on pharmaceuticals. It is an exciting new technology capable of providing insight into the structure and function of modern solid dosage forms. It combines the capability of spectroscopy for molecular analysis with the power of visualization affording precise characterization of the chemical composition, domain structure, and chemical architecture. In addition, this technique delineates the spatial uniformity of the active as well as each excipient across the final dosage form — features that may affect product performance. As demonstrated in this report, NIR spectral imaging was capable of distinguishing between various grades of blending in the final dosage form. It is recognized that the scale of scrutiny in this study was less than 1 unit. Additional investigations are planned to address the industrial/regulatory applications of this technique. The technique has much potential for a variety of applications in product quality assurance and could significantly enhance the manufacturing process. It is likely that it will be widely adopted and deployed in pharmaceutical analysis in the future and is particularly applicable to new product formulations and for understanding manufacturing defects.

ACKNOWLEDGEMENTS

The opinions expressed in this article are those of the authors and do not necessarily reflect the views and policies of the U.S. Food and Drug Adminstration. The authors would like to thank Alan S. Carlin (FDA) for assistance with tablet preparation and Christopher D. Ellison (FDA), Emil W. Ciurczak, and Linda H. Kidder (Spectral Dimensions) for technical advice and helpful discussions in support of this work.

REFERENCES

1. Blanco M, Coello J, Iturriaga H, Maspoch S, de la Pezuela C. Near-infrared spectroscopy in the pharmaceutical industry. Analyst. 1998;123:135R-150R.

2. Bugay DE. Characterization of the solid-state: spectroscopic techniques. Adv Drug Deliv Rev. 2001;48:43-65.

3. Wargo DJ, Drennen JK. Near-infrared spectroscopic characterization of pharmaceutical powder blends. J Pharm Biomed Anal. 1996;14:1415-1423.

4. Hailey PA, Doherty P, Tapsell P, Oliver T, Aldridge PK. Automated system for the on-line monitoring of powder blending processes using near-infrared spectroscopy. Part I. System development and control. J Pharm Biomed Anal. 1996;14:551-559.

5. Sekulic SS, Ward II HW, Brannegan DR, et al. On-line monitoring of powder blend homogeneity by near-infrared spectroscopy. Anal Chem. 1996;68:509-513.

6. El-Hagrasy AS, Morris HR, D'Amico F, Lodder RA, Drennen JK. Near-infrared spectroscopy and imaging for the monitoring of powder blend homogeneity. J Pharm Sci. 2001;90:1298-1307.

7. Delhaye M, Dhamelincourt P. Raman microprobe and microscope with laser excitation. J Raman Spectrosc. 1975;3:33-43.

8. Treado PJ, Morris MD. Infrared and Raman Spectroscopic Imaging. In: Morris MD, ed. Microscopic and Spectroscopic Imaging of the Chemical State, Practical Spectroscopy Series. Vol 16. New York, NY: Marcel Dekker; 1993:71-108.

9. Harthcock MA, Atkin SC. Imaging with functional group maps using infrared microspectroscopy. Appl Spectrosc. 1988;42:449-455.

10. Krishan K, Powell JR, Hill SL. Infrared microimaging. In: Humecki HJ, ed. Practical Guide to Infrared Microspectroscopy. New York, NY: Marcel Dekker; 1995:85-110.

11. Gat N. Imaging spectroscopy using tunable filters: a review. Proc SPIE-Int Soc Opt Eng. 2000;4056:50-64.

12. Schaeberle MD, Morris HR, Turner JF, Treado PJ. Raman chemical imaging spectroscopy. Anal Chem. 1999;5:175A-181A.

13. Treado PJ, Levin IW, Lewis EN. High fidelity Raman imaging spectroscopy: a rapid method using an acousto-optic tunable filter. Appl Specrosc. 1992;46:1211-1216.

14. Treado PJ, Levin IW, Lewis EN. Indium antimonide (InSb) focal plane array (FPA) detection for near-infrared imaging microscopy. Appl Specrosc. 1994;48:607-615.

15. Tran CD, Cui Y, Smirnov S. Simultaneous multispectral imaging in the visible and near-infrared region: applications in document authentication and determination of chemical inhomogeneity of copolymers. Anal Chem. 1998;70:4701-4708.

16. Lewis EN, Treado PJ, Reeder RC, et al. Fourier transform spectroscopic imaging using an infrared focal-plane array detector. Anal Chem. 1995;67:3377-3381.

17. Kidder LH, Levin IW, Lewis EN, Kleiman VD, Heilweil EJ. MCT focal-plane array detection for mid-infrared FT spectroscopic imaging. Opt Lett. 1997;22:742-744.

18. Lewis EN, Carroll JE, Clarke F. A near-infrared view of pharmaceutical formulation analysis. NIR News. 2001;12:16-18.

19. Zugates CT, Treado PK. Raman chemical imaging of pharmaceutical content uniformity. Int J Vibr Spectrosc. 1999;2:4. Availible at: www.ijvs.com.

20. Breitenbach J, Schrof W, Neumann J. Confocal Raman-spectroscopy: analytical approach to solid dispersions and mapping of drugs. Pharm Res. 1999;16:1109-1113.

21. The use of stratified sampling of blend and dosage units to demonstrate adequacy of mix for powder blends. Availible at: http://www.pqri.org/datamining/imagespdfs/bua052601pr.pdf.